Chemical Engineering Journal 157 (2010) 434–442

Contents lists available at ScienceDirect

Chemical Engineering Journal

journal homepage: www.elsevier.com/locate/cej

A comparative study on the kinetics and mechanisms of removal of Reactive Black 5 by adsorption onto activated carbons and bone char

Alvin W.M. Ip, John P. Barford, Gordon McKay*

Department of Chemical and Biomolecular Engineering, Hong Kong University of Science and Technology, Clear Water Bay, Kowloon, Hong Kong

ARTICLE INFO

Article history:
Received 4 March 2009
Received in revised form
26 November 2009
Accepted 3 December 2009

Keywords:
Adsorption
Kinetics
Reactive Black 5
Bamboo activated carbon
Bone char
Intraparticle diffusion

ABSTRACT

The adsorption of a large reactive dye, Reactive Black 5, onto four adsorbents has been studied. A commercial active carbon, F400, was selected as a standard and two active carbons prepared from bamboo, a biomaterial. The two bamboo derived carbons, BACX2 and BACX6 had high specific surface areas, namely, 2123 and 1400 m^2/g, respectively. A fourth widely used adsorbent, bone char, was also tested. The adsorption capacities for F400, bone char, BACX2 and BACX6 were 198, 160, 286 and 473 mg/g, respectively. A series of batch kinetics were carried out to investigate the rate and possible mechanism of Reactive Black 5 adsorption. Two pseudo-kinetic models and one intraparticle diffusion model were tested. The experimental concentration versus time decay curves were best explained by the intraparticle diffusion model.

1. Introduction

The textile industry discharges well over 150 million cubic metres of coloured effluents annually. The total annual world production of dyes is over seven hundred and thousand tonnes of which approximately 2% dyes are discharged in effluents [1]. In addition to the detrimental aesthetic effects of dyes in wastewaters, some dyes are toxic and/or carcinogenic [2,3]. Reactive acidic dyes are widely used due to the increasing use of cellulosic fibres [4]. Common methods for the treatment of textile effluents include adsorption, coagulation, advanced oxidation, flocculation and biological treatment. Adsorption is growing in popularity due to its potential for rapid treatment and the fact that it can produce a very high quality treated water. There is now a continuous search for adsorbents of different abilities for different treatment processes in an economic and sustainable manner [5].

Adsorption processes were always characterized by the adsorption kinetics and an adsorption isotherm. Both isotherm and kinetic data are important tools to understand the mechanisms of adsorption and are necessary for the design of adsorption treatment plant. In the present work, the adsorption of a large reactive acidic dye, namely, Reactive Black 5 onto four adsorbents—bone char, active carbon Filtrasorb F400 and two novel bamboo derived activated carbons, has been studied. The kinetic adsorption data on the dye removal on bamboo activated carbons and bone char is still limited although they have already shown good capacities for dye removal [6]. Commercial activated carbon F400 was selected in the present study as it has been extensively studied for dye and organic removal [7] and would be used as the model adsorbent for comparative purpose. The characteristics of the two bamboo derived activated carbons are reported. Equilibrium isotherm and batch kinetics studies of Reactive Black 5 adsorption on the four adsorbents have been studied and analyzed.

2. Equilibrium isotherm and batch adsorption kinetics models

2.1. Equilibrium isotherm

The adsorption capacity of adsorbents is one of the most important criteria to assess the performance of the adsorbents. The most convenient and direct way to investigate the adsorption capacity for an adsorbent to an adsorbate is to conduct an equilibrium isotherm study. When the amount of solute being adsorbed onto the adsorbent is equal to the amount being desorbed, equilibrium is established and the equilibrium solution concentration remains unchanged. Plotting solid phase concentration against liquid phase concentration graphically depicts the equilibrium isotherm. Adsorption behaviour has been successfully described by several equilibrium models [8]. Table 1 summarises the name

* Corresponding author. Tel.: +852 2358 8412; fax: +852 2358 0054.
E-mail address: kemckayg@ust.hk (G. McKay).

1385-8947/$ – see front matter © 2009 Elsevier B.V. All rights reserved.
doi:10.1016/j.cej.2009.12.003

Nomenclature

q_e	amount of adsorbate adsorbed at equilibrium ($mg\,g^{-1}$)
q_t	amount of adsorbate adsorbed at any time t ($mg\,g^{-1}$)
a_F	Freundlich isotherm constant ($L^{b_F}\,mg^{1-b_F}\,g^{-1}$)
a_L	Langmuir isotherm constant ($L\,mg^{-1}$)
a_{LF}	Langmuir–Freundlich isotherm constant [$(L/mg)^{bLF}$]
a_R	Redlich–Peterson isotherm constant [$(L/mg)^{bRP}$]
b_F	Freundlich isotherm exponent
b_R	Redlich–Peterson isotherm exponent
C_0	initial concentration of adsorbate in solution ($mg\,L^{-1}$)
C_e	equilibrium concentration of adsorbate in solution ($mg\,L^{-1}$)
k_1	pseudo-first-order rate constant (min^{-1})
k_1	pseudo-second-order rate constant ($g\,mg^{-1}\,min^{-1}$)
k_i	intraparticle diffusion rate constant ($mg\,g^{-1}\,min^{-0.5}$)
K_L	Langmuir isotherm constant ($L\,g^{-1}$)
K_{LF}	Langmuir–Freundlich isotherm constant ($L^{nLF}\,mg^{1-nLF}\,g^{-1}$)
K_R	Redlich–Peterson isotherm constant ($L\,g^{-1}$)
n_{LF}	Langmuir–Freundlich isotherm exponent
R^2	correlation coefficient
P	percentage of deviation (%)
V	volume of dye solution (L)
m	mass of adsorbent (g)
N	number of experimental data points

of isotherms and the corresponding mathematical formulas. The isotherm constants were determined by minimizing the difference between experimental and theoretical data using the normalised percentage of deviation (P%). The percentage of deviation can provide a good method for comparison between different systems when correlation coefficient (R^2) cannot be applied. The percentage of deviation was calculated by using the following equation:

$$P(\%) = \frac{100}{N} \times \sum_{i=1}^{N} \left| \frac{q_{e,cal} - q_{e,\exp}}{q_{e,\exp}} \right|_i \quad (1)$$

2.2. Batch adsorption kinetics

In order to investigate the mechanism of adsorption and potential rate controlling steps such as chemical reaction, diffusion control and mass transport processes, kinetic models have been used to test experimental data. The kinetic models for batch adsorption can be divided into two categories: (i) pseudo-kinetic chemical reaction controlled models and (ii) mass transfer controlled models. These are described below.

Table 1
Adsorption isotherm models and the corresponding equations.

Isotherm model	Equation		Reference
Freundlich isotherm	$q_e = a_F C_e^b$	(2)	[9]
Langmuir isotherm	$q_e = \frac{K_L C_e}{1 + a_L C_e}$	(3)	[10]
Redlich–Peterson isotherm	$q_e = \frac{K_R C_e}{1 + a_R C_e^{b_R}}$	(4)	[11]
Langmuir–Freundlich isotherm	$q_e = \frac{K_{LF} C_e^{n_{LF}}}{1 + a_{LF} C_e^{n_{LF}}}$	(5)	[12]

2.3. Pseudo-first-order kinetic model

Lagergren [13] proposed a rate equation for the sorption of solute from a liquid solution based on the adsorption capacity. The Lagergren equation is the most widely used rate equation in liquid phase sorption and this kinetic model is expressed as:

$$\frac{dq_t}{dt} = k_1(q_e - q_t) \quad (6)$$

Integrating the above equation for the boundary conditions $t = 0$ to $t = t$ and $q_t = q_t$ gives:

$$\ln(q_e - q_t) = \ln q_e - k_1 t \quad (7)$$

The kinetic constant k_1 can be determined by plotting $\ln(q_e - q_t)$ against t, or $\ln(q_e - q_t)/q_e$ versus t.

2.4. Pseudo-second-order kinetic model

Ho and McKay [14,15] developed a second-order equation based on adsorption capacity. This kinetic model can be written as:

$$\frac{dq_t}{dt} = k_2(q_e - q_t)^2 \quad (8)$$

Integrating the above equation for the boundary conditions $t = 0$ to $t = t$ and $q_t = 0$ to $q_t = q_t$ gives:

$$\frac{1}{q_e - q_t} = \frac{1}{q_e} + k_2 t \quad (9)$$

where k_2 is the pseudo-second-order rate constant of sorption. A linear form of this equation was shown as:

$$\frac{t}{q_t} = \frac{1}{k_2 q_e^2} + \frac{1}{q_e} t \quad (10)$$

If the pseudo-second-order equation is applicable, the plot of t/q_t against t of the above equation should give a linear relationship. This equation provides an advantage that the adsorption capacity of q_e can be obtained from the slope of the linear plot. The applications of this model are widely used in fitting the kinetic data for various systems [14].

2.5. Intraparticle diffusion model

Theoretical treatments of intraparticle diffusion yield rather complex mathematical relationships which differ in form as functions of the geometry of the sorbent particle. A functional relationship common to most treatments of intraparticle diffusion is that uptake varies almost proportionately with the halfpower of time, $t^{0.5}$, rather than t; nearly linear variation of the quantity sorbed with $t^{0.5}$ is predicted for a large initial fraction of reactions controlled by rates of intraparticle diffusion. Good linearization of the data is observed for the initial phase of the reaction in accordance with expected behaviour if intraparticle diffusion is the rate-limiting step [16]. The intraparticle diffusion equation is the following:

$$q_t = k_i t^{0.5} \quad (11)$$

where k_i is the intraparticle diffusion rate constant, $mg\,g^{-1}\,min^{-0.5}$. The k_i values under different conditions were calculated from the slopes of the straight line portions of the respective plots. The plot of q_t versus $t^{1/2}$ may present multi-linearity [17], which indicates that two or more rate controlling steps occur in the adsorption processes.

3. Materials and methods

3.1. Materials

C.I. Reactive Black 5 (colour index), chemical formula equal to $C_{26}H_{21}N_5Na_4O_{19}S_6$, FW = 991.82 g/mol, and λ_{max} = 599 nm was obtained from International Laboratory (USA). One thousand milligram per litre stock solution was prepared by dissolving the required amount of dye in deionised water. The working solution was prepared by diluting the stock solution into the desired concentrations. The structure of the dye is produced by ChemDraw and shown in Fig. 1.

The bamboo activated carbons were produced by chemical activation of crushed bamboo scaffolding wastes by phosphoric acid. The production process is reported elsewhere [18]. Two bamboo activated carbons with impregnation ratio (X_p) of 2 and 6, namely BACX2 and BACX6, were used as adsorbents in this study. Granular activated carbon Filtrasorb 400 (F400) was purchased from Calgon Carbon Corporation, USA. Bone char Brimac 216 is another adsorbent purchased from Brimac Charcoals Limited, UK. The adsorbents were oven dried at 105 °C for 24 h and stored in desiccator until used. The particle size of adsorbent used in this study was 180–355 μm.

3.2. Chemical and physical characterizations of the adsorbents

The surface acidic and basic function groups were determined by Boehm titration method [19]. For the measurement of surface acidity, 0.2 g of adsorbents were contacted with 50 mL of 0.05N standard NaOH and shaken for 2 days. The mixture was filtered and then back-titrated with 0.05N standard HCl. For the measurement of surface basicity, 0.2 g of adsorbents were contacted with 50 mL of 0.05N standard HCl and shaken for 2 days. The mixture was filtered and then back-titrated with 0.05N standard NaOH. Mass titrations were employed to determine the point of zero charge of the adsorbents [6]. The textural properties were performed by determining the nitrogen adsorption/desorption isotherms at 77 K using a Quantachrome Autosorb 1. The specific surface area was calculated using the BET equation (S_{BET}) from the adsorption data of N_2 at 77 K. The pore size distribution was calculated using the Barrett, Joyner and Halenda (BJH) model. The micropores and mesopores volumes were calculated using alpha-s method and BJH method, respectively.

3.3. Adsorption isotherm study

Reactive Black 5 (RB 5) is used to investigate the adsorption capacity of the four different adsorbents. A constant mass of adsorbent (0.05 g) was weighed into 60 mL glass bottles and contact with 50 mL of dye solutions of different initial concentrations. The bottles were sealed and placed in a shaker until equilibrium is reached. Upon equilibration, samples were analyzed to determine the residual equilibrium liquid phase dye concentration.

3.4. Batch kinetic study

These experiments were used to investigate the influence of initial concentration and adsorbents on the adsorption rate. An adsorber vessel in a batch stirred bank configuration was used in all of the experiments. The design of the standard agitated batch adsorber has been described in previous paper [20]. About 0.85 or 1.275 g of adsorbents was mixed with 1700 mL dye solution in batch system for 72 h. The impeller speed was 400 rpm and the temperature was kept at 25 ± 1 °C. A range of dye concentrations (50, 100, 150, 200 mg/L) were used to investigate the sorption of dye onto the adsorbents. At time = 0 and selected time intervals, 4 mL samples were extracted from the vessel using a 10 mL syringe.

3.5. Measurement of dye uptake

The concentration of the dyes was determined by measuring the absorbance of the samples at the absorbance maximum wavelength (λ_{max}) by Varian Cary IE spectrophotometer. The liquid phase dye concentration was measured at different time intervals and equilibrium is reached when the adsorption capacity of the adsorbent remains constant. The equilibrium adsorption capacity, q_e (mg/g), at different dye concentrations was determined by a mass balance on the dye:

$$q_e = \frac{V(C_0 - C_e)}{m} \tag{12}$$

where C_0 (mg/dm^3) is the initial concentration, C_e (mg/L) is the equilibrium concentration in the liquid phase, V is the volume of liquid phase (L), and m is the mass of the absorbent (g). The plot of equilibrium adsorption capacity against equilibrium concentration in the liquid phase graphically depicts the equilibrium isotherm.

4. Results and discussion

4.1. Chemical and physical characterization of the adsorbents

The textural characteristics of the adsorbents calculated from the results of nitrogen adsorption isotherm at 77 K are shown in Table 2 and the pore size distribution of the adsorbents is shown in Fig. 2. As can be seen from the results, the adsorbents are varied in their physical structure. Both bamboo activated carbons have a higher surface area than the other adsorbents. BACX2 (based on X_p = 2) gives the high surface area and micropore volume, whereas,

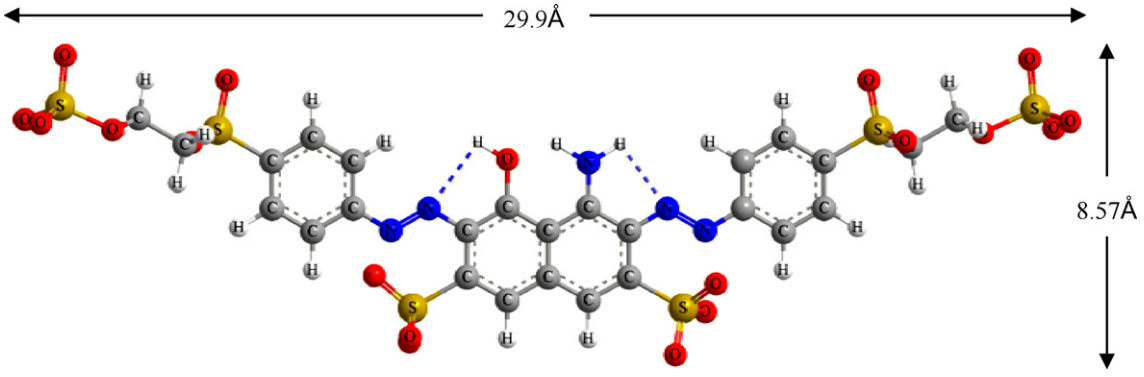

Fig. 1. Molecular structure of the Reactive Black 5.

Table 2
BET surface area, pore volume and the average diameters of the four adsorbents.

Adsorbent	BET surface area (m^2/g)	Micropore volume (cm^3/g)	Mesopore volume (cm^3/g)	Average pore diameter (nm)
F400	793	0.363	0.123	2.44
Bone char	107	0	0.255	9.43
BACX2	2123	0.494	0.943	2.79
BACX6	1400	0.209	2.008	5.32

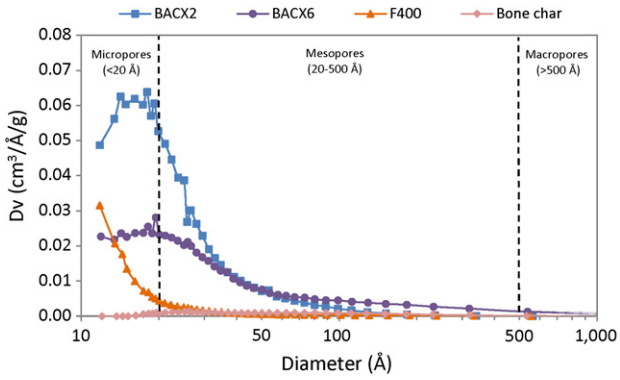

Fig. 2. Pore size distribution of the adsorbents.

BACX6 (based on $X_p = 6$) has the highest mesopore volume. It was found that the impregnation ratio greatly affected the surface area and the pore structure of the bamboo activated carbon [18]. Increasing the impregnation ratio can widen the pore of the activated carbon, indicated by the shift to the right in the pore size distribution of bamboo activated carbons (Fig. 2). All three types of pores, micopores (<2 nm), mesopores (2–50 nm) and macropores (>50 nm), existed in the BACX6. F400 is a predominately microporous material and the percentages of micropore and mesopore volume of F400 are 58% and 42%, respectively. Bone char has a low surface area as it is produced from the calcination of bone at 1000 °C in the absence of oxygen and it appears that bone char comprises only mesopores. The chemical characteristics of the adsorbents were also studied and the point of zero charge, total acidic groups and basic groups of the adsorbents were summarised in Table 3.

4.2. Equilibrium adsorption

Adsorption isotherms describe the non-linear and dynamic equilibrium between the adsorbed solute on the adsorbent (mg/g) and solute in the solution (mg/L) at a constant temperature. The equilibrium liquid phase concentration (C_e) for different adsorbents was measured and their adsorption capacity (q_e) was calculated. The results which are expressed as plots of solid phase dye concentration against liquid phase dye concentration are shown in Fig. 3. It can be seen that BACX6 has a much higher adsorption capacity than the other absorbents. The adsorption capacity of F400 is slightly higher than that of bone char. Both F400 and bone char have a higher adsorption capacity than BACX2 when the equilibrium liquid phase concentration is low, whereas, the adsorption capacity of F400, bone char and BACX2 is comparable when the equilibrium liquid phase concentration is high. Ip et al. [18] studied the adsorption of Acid Red 18 which is an anionic dye with a smaller size when comparing with Reactive Black 5. It was found the adsorption capacity of F400 is much higher than that of bone char.

Table 3
Acidity, basicity and point of zero charge (pH_{pzc}) of the four adsorbents.

Adsorbent	Total acidic groups (mmol/g)	Total basic groups (mmol/g)	pH_{pzc}
F400	0.40	0.42	7.33
Bone char	0.13	3.07	9.83
BACX2	2.52	0.05	1.84
BACX6	2.50	0.15	1.93

To optimise the design and the operation of an adsorption system, it is important to correlate the experimental results to a theoretical model or empirical equation. Therefore, the experimental data were fitted to the Langmuir, Freundlich, Redlich–Peterson (R–P) and Langmuir–Freundlich (L–F) isotherm models which are the most common two-parameter and three-parameter equations in the literature. A minimizing procedure was adopted to solve the equation by using Eq. (1). Table 4 summarises the corresponding constant for each system and Fig. 3 presented the best fit isotherm model of the adsorbents. By comparing the results of the values of P (%), the L–F isotherm results in the lowest value of P (%) for adsorption of RB 5 by F400 and bone char, whereas, the R–P isotherm results in the lowest values of P (%) for the adsorption of RB 5 by bamboo activated carbons. The best fit L-F isotherm for F400 and bone char may suggest a dissociative adsorption process. More than one site could be occupied by the Reactive Black 5 as there are four sulphonate ions in the structure of Reactive Black 5. The carboxylic group and phenolic groups are present in the activated carbon and they may be responsible for forming hydrogen bonds with dye molecules. There are number of functional groups in the dye molecules that can form hydrogen bonds and these include: $-NH_2$, –S=O, –O–H. The best R–P isotherm for bamboo activated carbons may imply that the mechanism of RB 5 adsorption is a hybrid which combines the elements from both the Langmuir and Freundlich equation and does not follow ideal monolayer adsorption.

4.3. Kinetics of adsorption

A series of kinetic studies have been performed on all four adsorbents using four initial dye concentrations. The experimental

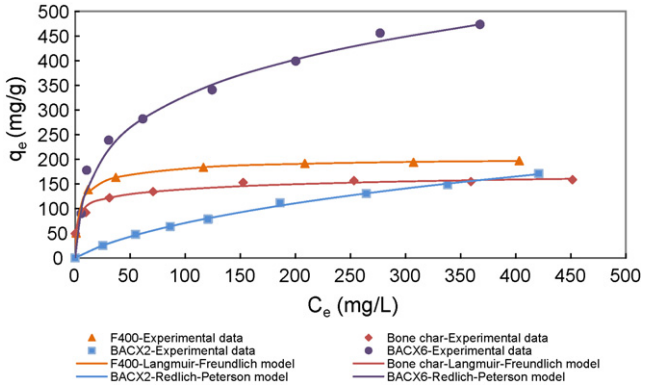

Fig. 3. Adsorption isotherm of Reactive Black 5 for different adsorbents with their best fitting models.

Table 4
Isotherm constants for Reactive Black 5 using different models.

	Adsorbents			
	F400	Bone char	BACX2	BACX6
Langmuir isotherm				
K_L	29.87	22.42	1.001	20.74
a_L	0.15	0.14	0.0036	0.047
q_e (mg/g)	197.5	160.0	281.2	441.7
P (%)	9.18	13.86	4.23	9.52
Freundlich isotherm				
a_F	66.61	66.02	3.954	76.24
b_F	0.20	0.15	0.62	0.31
P (%)	11.05	4.23	3.73	8.79
Redlich–Peterson isotherm				
K_R	101.2	1490	1.383	35.97
a_R	0.77	19.23	0.05	0.29
b_R	0.93	0.87	0.65	0.76
P (%)	4.26	4.00	**1.54**	**5.58**
Langmuir–Freundlich isotherm				
K_{LF}	77.57	106.7	2.200	35.63
a_{LF}	0.37	0.44	0.0043	0.051
n_{LF}	0.63	0.27	0.79	0.63
P (%)	**2.84**	**2.90**	2.23	6.34

The bold values mean that it has the lowest P (%) value when it is compared with other models.

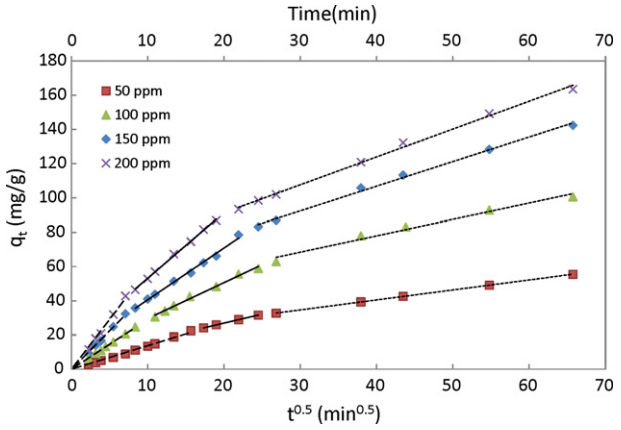

Fig. 4. Root time plot for the adsorption of Reactive Black 5 onto BACX6.

concentration versus time data is presented in Figs. 4–7 for F400, bone char, bamboo activated carbon BACX2 and BACX6, respectively. The kinetic data have been analyzed using three models: a pseudo-first-order kinetic model, a pseudo-second-order kinetic model and an intraparticle diffusion model.

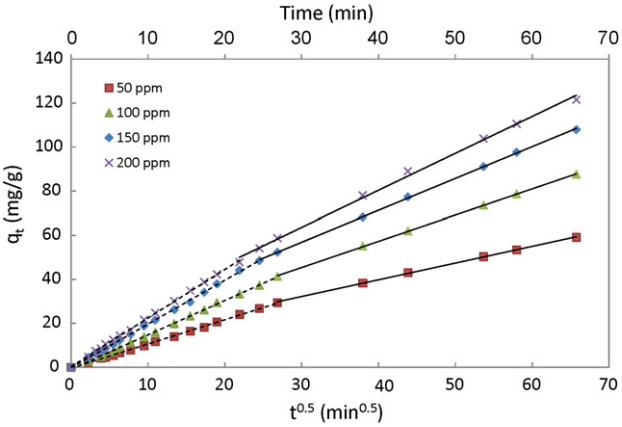

Fig. 5. Root time plot for the adsorption of Reactive Black 5 onto F400.

4.3.1. Pseudo-first-order and pseudo-second-order kinetic modelling

Table 5 presents the values of constants of the pseudo-first-order and pseudo-second-order kinetic models for adsorption of Reactive Black 5 onto the four selected adsorbents. The value of the correlation coefficient (R^2) obtained from the linear plot of pseudo-first-order kinetic model (Eq. (7)) was relatively small for the F400, BACX2 and BACX6 studied at different initial concentrations and the experimental q_e values were larger than the calculated values, $q_{e,cal}$, from the linear plots. However, the linear plot of pseudo-first-order kinetic model on bone char was relatively high, which ranged from 0.97 to 0.98. The fits of the experimental data with the pseudo-second model data are better than pseudo-first-order model for other systems including F400, BACX2 and BACX6 as the models have higher values of R^2 which varied from 0.96 to 0.99. However, the values of $q_{e,cal}$ calculated from the slopes of the linear plots of the pseudo-second-order kinetic model (Eq. (10)) were significantly deviated from the values of experimental q_e. Good matches for these two values have been reported by a number of workers [21–23]. It seems that the pseudo-first-order and pseudo-second-order model are not suitable to describe the adsorption of Reactive Black 5 onto the activated carbons and bone char.

4.4. Intraparticle diffusion

The mechanism of adsorption is generally considered to involve: (i) mass transfer of adsorbate from the bulk phase to particle surface, (ii) adsorption at a site on the surface and (iii) intraparticle diffusion of the adsorbate molecules to an adsorption site either by a pore diffusion process (by either pore diffusion and/or surface diffusion mechanism). Step (ii) is often assumed to be extremely rapid, thus the adsorption of large molecules, with long contact times to equilibrium, is always considered to be diffusion controlled by external film resistance and/or internal diffusion mass transport or intraparticle diffusion [16]. However, the above kinetics models were not able to identify the mechanism of adsorption of RB 5 onto the activated carbons and bone char. Generally, the rate of adsorption is limited by external mass transfer for a system with poor mixing, low adsorabate concentration, high affinity to adsorbent and small particles. In this study, the adsorption was conducted in a well agitated tank and RB 5 is a large molecule with a long contact time to reach equilibrium. Therefore, it is proposed that the rate of adsorption is governed by the intraparticle diffusion in the pore structure.

A classical approach to analyze if an adsorption process is controlled by intraparticle diffusion is to plot the amount adsorbed versus the square root of time, $t^{0.5}$ (Figs. 4–6). The intraparticle rate constant at different initial concentrations obtained from the slope of the plots was summarised in Table 6. If the plot is linear

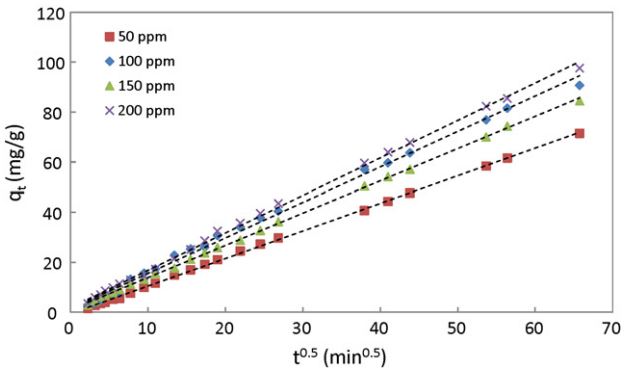

Fig. 6. Root time plot for the adsorption of Reactive Black 5 on bone char.

Table 5
Calculated and experimental q_e values and the pseudo-first- and pseudo-second-order rate constants.

Adsorbents	Initial concentration (C_0)	$q_{e,exp}$ (mg/g)	$q_{e,cal}$ (mg/g)	k_1 (min^{-1})	R^2	$q_{e,cal}$ (mg/g)	k_2 (g/(mg min))	R^2
F400	50	94.3	83.2	0.000226	0.955	61.0	0.0000314	0.968
	100	151.9	137.9	0.000194	0.953	90.9	0.0000192	0.962
	150	174.0	156.1	0.000218	0.954	109.9	0.0000187	0.963
	200	182.9	166.2	0.000210	0.954	123.5	0.0000170	0.963
Bone char	50	88.0	88.9	0.000296	0.985	72.5	0.0000211	0.940
	100	122.1	112.5	0.000243	0.974	84.7	0.0000207	0.937
	150	135.7	122.6	0.000253	0.967	91.7	0.0000201	0.954
	200	143.9	128.6	0.00026	0.976	95.2	0.0000201	0.946
BACX2	50	28.7	26.1	0.000153	0.901	14.2	0.000170	0.967
	100	52.5	46.7	0.000162	0.879	27.0	0.000104	0.975
	150	70.8	62.5	0.000131	0.839	31.7	0.000113	0.982
	200	87.9	76.6	0.000115	0.792	36.6	0.000120	0.984
BACX6	50	92.8	79.5	0.000204	0.824	50.3	0.0000758	0.984
	100	173.1	147.1	0.000202	0.830	102.0	0.0000362	0.987
	150	232.9	194.7	0.000210	0.848	142.9	0.0000244	0.983
	200	280.9	231.2	0.000185	0.797	192.3	0.0000184	0.988

and passes through the origin, it is indicative that intraparticle diffusion is controlling the rate of adsorption. Some authors [24,25] have shown that if there is an initial external mass transfer or chemical reaction, then the slope will still be linear but that it will not pass through the origin. Figs. 4 and 5 show the root time plots for the adsorption of RB 5 onto the bamboo derived activated carbon BACX6 and F400 at different initial concentrations. All the plots exhibited multi-linearity and the correlation coefficients (R^2) for the intraparticle diffusion are (>0.995), indicating that more than one diffusion step took place.

Fig. 4 clearly shows the three linear sections; indicating intraparticle diffusion controlled by the three pore size ranges. The slope of the linear portion indicated the rate of the adsorption process. The result showed the diffusion rates decreased with increasing the contact time. Since the dye molecules diffuse into the inner structure of the adsorbents, the pores for diffusion become smaller. Therefore, the free path of the molecules in the pore decreases and the molecules may also be blocked. Other authors [17,26] have also identified three linear sections on the root time plot and these have been attributed to the three pore regions macropores, mesopores and micropores. However, we now consider this to be incorrect. The fraction surface area in the macropores is usually 1% or less of the total surface area. However, the fractional uptake of dye in the first linear region is always greater than 10% of the equilibrium value and sometimes as high as 25%. This first linear region is most likely due to the adsorption to the mesopores as it is not reasonable that the small surface area in the macropores can adsorb more than 10% of dye molecules. This is supported by the high average pore diameter value in Table 1. Three linear sections can also be observed from intraparticle plots of BACX6 in Fig. 4 and for BACX2 (data not shown). The last linear section of the plots yielding three linear sections in the microporous region and for the adsorption of RB 5 these pores are the supermicropores, i.e. d_{pore} = 7.0–20 Å. Adsorption of solute molecules can take place in pore diameters of 1.3–1.8 times the solute molecular width [27] or 1.7 times the solute molecular width [28]. Therefore, if we assume a value of 1.6 times the molecular width, this implies a minimum pore adsorbing diameter from Fig. 1 of 1.6 × 8.57 = 13.7 Å. The shortest side of the dye molecules, that is, 8.57 Å, was selected because most of dye molecules probably diffuse into the porous structure of adsorbent through the longitudinal position as suggested by Giles et al. [29] and the diffusion is a random process. Therefore, the diffusion is restricted by the shortest side of dye molecule. Consequently there will be some adsorption into the supermicropores. The assignment of the second linear section is not obvious but it is likely to represent the transition region from mesopores to micropores. This 'transit' can also be observed in α-plots and t-plots [30–32], widely used for determining micropore and mesopore surface areas and volumes by nitrogen adsorption isotherm. The linear plots used for these parameter estimations do not pass clearly through the experimental data points [33–35] at the point of intersection corresponding to a pore diameter of 20 Å. The experimental data points of the α-plots and t-plots in this region, that is, 20 ± 4 Å, are curved and represent a transition region corresponding to the second linear region of the root t-plots in Fig. 4.

There are two aspects relating to the explanation of the two linear sections only in Fig. 5. The first linear section is probably the diffusion in the mesopores and meso–micropores transition region and corresponds on average to about 15% (w/w) of the F400 equilibrium uptake of RB 5. To explain the second linear section and the absence of the third linear section is linked to the diffusion rate and hence the mean pore size of F400 is shown in Table 2 as 24.4 Å whereas for BACX6 it is 53.2 Å, therefore RB 5 can penetrate BACX6

Table 6
The intraparticle rate parameters of different adsorbents and R^2 value for the root time plot.

Adsorbent				
F400				
C_0 (mg/L)	50	100	150	200
k_1 (mg g^{-1} min$^{0.5}$)	1.1093	1.5775	1.9811	2.2322
R^2	0.9991	0.9995	0.9990	0.9995
k_2 (mg g^{-1} min$^{0.5}$)	0.7424	1.1726	1.4562	1.6780
R^2	0.9999	0.9994	0.9990	0.9994
Bone char				
C_0 (mg/L)	50	100	150	200
k_1 (mg g^{-1} min$^{0.5}$)	1.1068	1.2880	1.4166	1.4967
R^2	0.9994	0.9996	0.9957	0.9985
BACX2				
C_0 (mg/L)	50	100	150	200
k_1 (mg g^{-1} min$^{0.5}$)	0.2662	0.6669	1.023	1.3282
R^2	0.999	0.9953	0.9928	0.9967
k_2 (mg g^{-1} min$^{0.5}$)	0.2371	0.4542	0.6376	0.8511
R^2	0.9967	0.9961	0.9939	0.9939
K_3 (mg g^{-1} min$^{0.5}$)	0.1247	0.2015	0.2987	0.3662
R^2	1	0.9975	0.9961	0.9947
BACX6				
C_0 (mg/L)	50	100	150	200
k_1 (mg g^{-1} min$^{0.5}$)	1.3739	2.9129	4.8086	6.4511
R^2	0.9931	0.9988	0.9941	0.9973
k_2 (mg g^{-1} min$^{0.5}$)	1.0461	2.1014	3.0262	3.8306
R^2	0.9999	0.9925	0.9938	0.9984
K_3 (mg g^{-1} min$^{0.5}$)	0.5848	0.9517	1.4381	1.6288
R^2	1.0000	0.9967	0.9961	0.9965

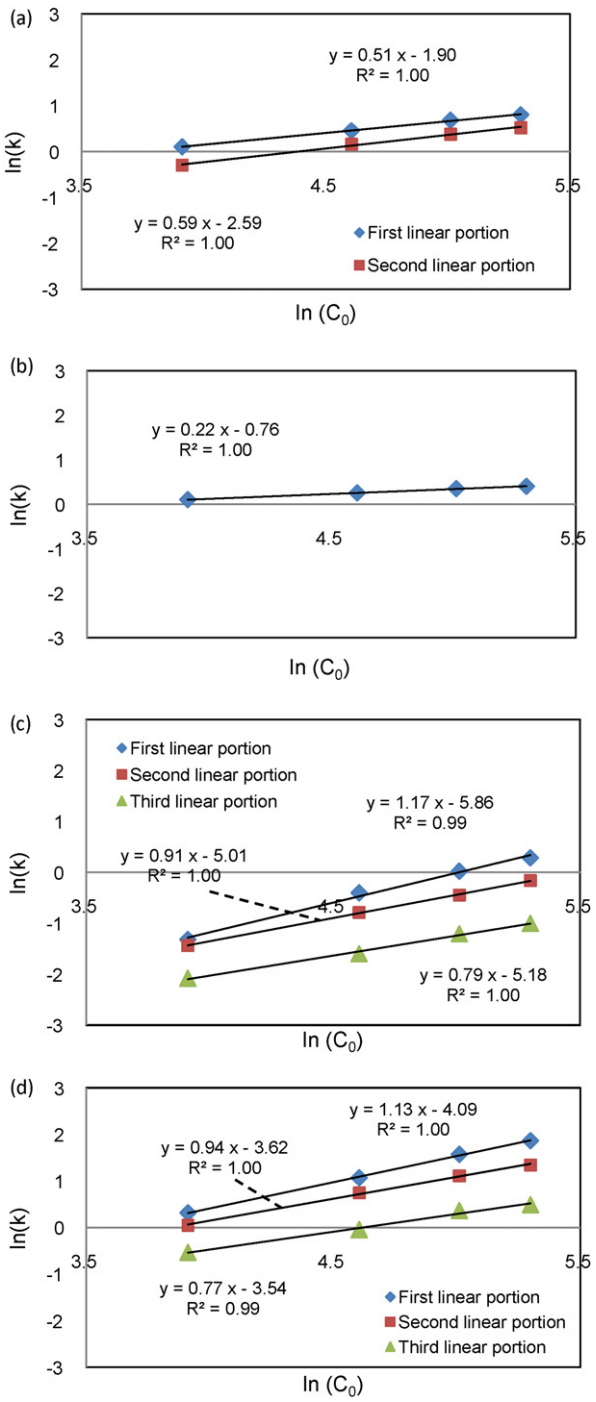

Fig. 7. The ln(k) versus ln(C_0) plots for (a) F400, (b) bone char, (c) BACX2 and (d) BACX6.

much faster. Consequently, the linear section responsible for the large mesopore is not apparent and Fig. 4 shows only two linear sections whose slopes are not too different reflecting the overall small mean pore diameter in F400. Therefore, based on the discussion in the previous section that the transition region pores in F400 are in the diameter range 20 ± 4 Å that is very close to micropores. It is likely that the adsorption of RB 5 on F400 in the second linear section is in the micropore region in Fig. 5, because many of the adsorbing micropores are in this region even after 400 min. The highest q_e value at 400 min in Fig. 5 is approximately 40 mg RB 5 per gram F400 and this is much lower than the q_e value for the same dye concentration in Fig. 4 for BACX6 at 400 min in the transitional region. The pure micropore adsorption region for F400 takes place after 400 min contact time.

Fig. 6 shows the root time plot for the adsorption of RB 5 on bone char. Only one linear section is observed over a wide time range. However, the surface area of bone char is very low, namely, 100 m^2/g (Table 2) and the average pore diameter in Table 1 is 94.3 Å. The bone char is predominantly composed of mesopores and consequently only shows one linear on the root t-plot. The intraparticle rate parameters, k_i, are shown in Table 6 together with R^2 values.

4.5. Effect of initial concentration

As can be seen in Table 7, increasing the initial concentration led to an increase of the intraparticle rate parameters in three portions as an increase in the concentration lead to increase of driving force of diffusion which depends on concentration gradient and the intraparticle diffusion model was developed base on Fick's Law. There is a correlation for the intraparticle rate parameters and the initial concentration and can be represented by following equation:

$$k_i = AC_0^B \tag{13}$$

Eq. (13) can be transformed to a linear Eq. (14)

$$\ln(k_i) = \ln(A_i) + B_i \ln(C_0) \tag{14}$$

The value of the exponent B is the slope of Fig. 7 and it determines the effect of concentration on the rate of intraparticle diffusion. The index i (1, 2, 3) corresponds to the first, second and third linear section in the root t-plot. The plots of log k_i versus log (C_0) are shown in Fig. 7 and the values of the correlation constants A and B are given in Table 7.

The theoretical equations for intraparticle diffusion indicate that the concentration dependence of a diffusion–adsorption process will vary depending on the characteristics of the adsorption isotherm and on the fraction of solute adsorbed at equilibrium. Eq. (13) can give an indication on how the intraparticle diffusion depends on the dye concentration. A value of 0.50–0.64 for the exponent B has been reported for adsorption of acid dyes on activated carbon by Choy et al. [16]. Similar value of exponent B for adsorption of Reactive Black 5 onto F400 was obtained in the present studies. However, a higher value of exponent B for adsorption onto BACX6 and a lower value of exponent B for adsorption onto bone char were obtained as the adsorbents studied are quite different in pore sizes and surface activities. The concentration has a much larger effect in the rate of intraparticle diffusion on bamboo activated carbon when it is compared with other adsorbents (larger value of B). It may due to the mechanism of adsorption of RB 5 onto the bamboo activated carbon. As the pH of the solution is higher than the point of zero charge of the bamboo activated carbon, the surface of the bamboo activated carbon would bring a negatively surface charged. The interaction between the RB 5 and the surface of the bamboo activated carbon is rather weak due to the electrostatic repulsions between the negatively charged RB 5 and the negatively charged surface of bamboo activated carbon. Therefore, increasing the concentration of RB 5 can enforce more dyes to adsorb onto the

Table 7
Correlation values for the effect of concentration.

	k_1		k_2		k_3	
	A_1	B_1	A_2	B_2	A_3	B_3
F400	0.150	0.511	0.075	0.591	N.A.	N.A.
Bone char	0.469	0.220	N.A.	N.A.	N.A.	N.A.
BACX2	0.003	1.169	0.007	0.914	0.006	0.788
BACX6	0.017	1.125	0.027	0.941	0.029	0.765

bamboo activated carbon and hence increase the driving force of diffusion.

4.6. Mechanism of adsorption and effect of pH

It is important to distinguish between the mechanism of adsorption, that is, the reaction at the surface, namely, physical or chemical sorption; and, the rate controlling mechanism. In most classical adsorption systems using microporous or mesoporous adsorbents, the rate controlling mechanism will be heavily dependent on either pore or surface diffusion. For macroporous adsorbents the rate controlling process will be the surface reaction. For the four adsorption systems reported in this paper, we will consider diffusion and the reaction chemistry of the dye–adsorbent interface and attempt to predict the mechanism of adsorption.

RB 5 is an acidic dye which ionises in water to form a negatively charged coloured ion.

$$DyeNa_4 \rightarrow Dye^{4-} + 4Na^+$$

Bone char consists primarily of apatite II (hydroxyapatite) and approximately 10% elemental carbon. The basic and acid sites are formed by the protonation and deprotonation of hydroxyl groups of hydroxyapatite on the surface of bone char [36]. The basic surface can be expressed as:

$$= Ca\text{–}OH + H^+ \rightarrow = Ca\text{–}OH_2{}^+$$

The acidic surface can be expressed as:

$$= P\text{–}OH \rightarrow = PO^- + H^+$$

where (=) represents the hydroxyapatite surface.

Therefore, there is attraction between the negative RB 5 dye ion and the bone char particle as there is some uptake of hydrogen ions into the bone char due to the protonation of hydroxyl groups (the solution pH rises as shown in Fig. 8). As the pH of the solution is lower than the point of zero charge of bone char, the surface of bone char would bring an overall negatively charge. In addition, about 10% of bone char is active carbon from the bone charring process at around 700 °C. The surface area, largely due to the active carbon is 100 m^2/g and the RB 5 dye ion can pass into these pores and physically adsorb on the carbon surface.

The pH profile for the adsorption of RB 5 onto F400 is shown in Fig. 8. The slightly increase in pH implied that the surface adsorbed more H^+ ion than OH^- ion and F400 exhibited a net positive charge which can help the adsorption of the negative portion of RB 5. In the case of adsorption by bamboo activated carbons, the solution pH dropped sharply to 3.4 and then become steady. The bamboo activated carbons carried negative charges which do not favor the adsorption of the negatively charged RB 5. Therefore, the surface charge on the activated carbons cannot be solely used to explain the mechanism of adsorption as the adsorption capacities are opposed to the explanation by surface charge.

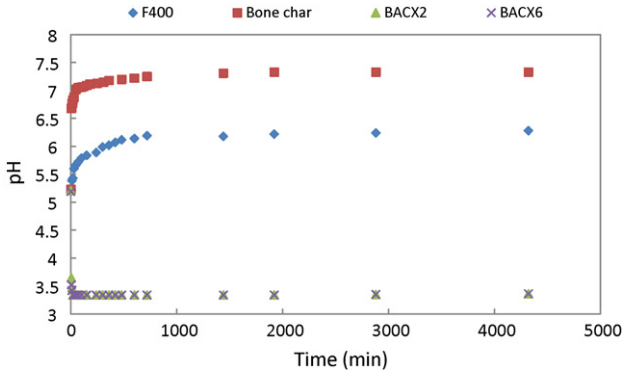

Fig. 8. pH profile of Reactive Black 5 adsorption onto F400, bone char, BACX2 and BACX6 (initial pH: 5.2, initial concentration: 50 mg/L, temperature: 25 °C, agitation rate: 400 rpm).

By considering the RB 5 adsorption capacities based on surface area and the micropore and mesopore diameters, the two bamboo derived active carbons the surface area ratio is 1.5:1 (BACX2:BACX6) and the ratio of adsorption capacities is 1:1.7, so the connection is very low. For F400, the surface area ratio is 1.75:1 for BACX6 to F400, whereas the adsorption capacity ratio is ≈2.25. That is, the capacity is much larger. In this case, pore diameter is very significant, as F400 has a high micropore content but a relatively low mesopore content compared to the two bamboo carbons. The mean average pore diameter, d_p, is 24.4 nm and for micropores d_p < 2 nm. The RB 5 is a large dye molecule as shown in Fig. 1 and a mesopore volume of 0.264 cm^3/g, therefore molecules will not be able to penetrate many of the micropores in F400, which is a highly microporous adsorbent. The two bamboo carbons have much higher mesopore volumes, namely, 0.943 and 2.008 cm^3/g for BACX2 and BACX6, respectively, and this would explain their much higher adsorption capacities. Al-Degs et al. [37] investigated the effect of particle size on the adsorption of reactive dyes onto F400 and found that adsorption capacity increased with a decrease in particle size. This can be attributed to the large molecular diameter of reactive dyes which did not penetrate the whole particle but instead adsorb near or on the carbon surface.

5. Conclusions

Based on the kinetics and diffusion analyses performed in this paper, it appears that the uptake of dye on all four adsorbents is by diffusion control. The mechanisms vary in that the uptake of Reactive Black 5 on bone char (SA: 100 m^2/g) shows only one rate controlling region on the root time plot, whereas the adsorption of Reactive Black 5 onto active carbon F400 and bamboo activated carbons, there are two and three linear controlling regions, respectively. There are three linear controlling regions in the bamboo activated carbons which are corresponding to the diffusion to the mesopores, transitional pores and micropores. Adsorption equilibrium data follows Redlich–Peterson isotherm equation with F400 and bone char while the data was fitted using Langmuir and Freundlich isotherm equation with the bamboo activated carbons.

References

[1] J.R. Easton, The dye maker's view, in: P. Cooper (Ed.), Colour in Dyehouse Effluent, Society of Dyers and Colourists, Bradford, England, 1995.
[2] M.A. Brown, S.C. DeVito, Predicting azo dye toxicity, Crit. Rev. Environ. Sci. Technol. 23 (1993) 249–324.
[3] A. Reife, H.S. Freeman, Environmental Chemistry of Dyes and Pigments, Wiley, New York, 1994.
[4] C. O'Neill, F.R. Hawkes, D.L. Hawkes, N.D. Lourenco, H.M. Pinheiro, W. Delee, Colour in textile effluents—sources, measurement, discharge consents and simulation: a review, J. Chem. Technol. Biotechnol. 74 (1999) 1009–1018.
[5] M. Valix, W.H. Cheung, G. McKay, Roles of the textural and surface chemical properties of activated carbon in the adsorption of acid blue dye, Langmuir 22 (2006) 4574–4582.
[6] A.W.M. Ip, J.P. Barford, G. McKay, Reactive Black dye adsorption/desorption onto different adsorbents: effect of salt, surface chemistry, pore size and surface area, J. Colloid Interface Sci. 337 (2009) 32–38.
[7] G. McKay, M.F.F. Sze, The removal of organic pollutants from industrial effluents via tapered bed adsorption columns, Int. J. Environ. Technol. Manage. 9 (2008) 20–33.
[8] S.J. Allen, G. McKay, J.F. Porter, Adsorption isotherm models for basic dye adsorption by peat in single and binary component systems, J. Colloid Interface Sci. 280 (2004) 322–333.
[9] H.M.F. Freundlich, Over the adsorption in solution, J. Phys. Chem. 57 (1906) 385–470.
[10] I. Langmuir, The adsorption of gases on plane surfaces of glass, mica and platinum, J. Am. Chem. Soc. 40 (1918) 1361.
[11] O. Redlich, D.L. Peterson, A useful adsorption isotherm, J. Phys. Chem. 63 (1959) 1024.

[12] R. Sips, Combined form of Langmuir and Freundlich equations, J. Phys. Chem. 16 (1948) 490–495.
[13] S. Lagergren, Zur Theorie der sogenannten adsorption geloster stoffe. Kungliga Sevenska Vetenskapsakademiens, Handlingar 24 (1898) 1–39.
[14] Y.S. Ho, G. McKay, Pseudo-second order model for sorption processes, Process Biochem. 34 (1999) 451–465.
[15] Y.S. Ho, G. McKay, The kinetics of sorption of divalent metal ions onto sphagnum moss peat, Water Res. 34 (2000) 735–742.
[16] K.K.H. Choy, J.F. Porter, G. McKay, Intraparticle diffusion in single and multicomponent acid dye adsorption from wastewater onto carbon, Chem. Eng. J. 103 (2004) 133–145.
[17] S.J. Allen, G. McKay, K.Y.H. Khader, Intraparticle diffusion of a basic dye during adsorption onto sphagnum peat, Environ. Pollut. 56 (1989) 39–50.
[18] A.W.M. Ip, J.P. Barford, G. McKay, Production and comparison of high surface area bamboo derived active carbons, Bioresour. Technol. 99 (2008) 8909–8916.
[19] H.P. Boehm, Some aspects of the surface chemistry of carbon blacks and other carbons, Carbon 32 (1994) 759–769.
[20] C.W. Cheung, J.F. Porter, G. McKay, Removal of Cu(II) and Zn(II) ions by sorption onto bone char using batch agitation, Langmuir 18 (2002) 650–656.
[21] I.A.W. Tan, B.H. Hameed, A.L. Ahmad, Equilibrium and kinetic studies on basic dye adsorption by oil palm fibre activated carbon, Chem. Eng. J. 127 (2007) 111–119.
[22] B.H. Hameed, I.A.W. Tan, A.L. Ahmad, Adsorption isotherm, kinetic modeling and mechanism of 2,4,6-trichlorophenol on coconut husk-based activated carbon, Chem. Eng. J. 144 (2008) 235–244.
[23] Z. Aksu, A.I. Tatli, O. Tunc, A comparative adsorption/biosorption study of Acid Blue 161: effect of temperature on equilibrium and kinetic parameters, Chem. Eng. J. 142 (2008) 23–39.
[24] B.H. Hameed, F.B.M. Daud, Adsorption studies of basic dye on activated carbon derived from agricultural waste: Hevea brasiliensis seed coat, Chem. Eng. J. (2008) 48–55.
[25] A. Khaled, A. El Nemr, A. El-Sikaily, O. Abdelwahab, Treatment of artificial textile dye effluent containing Direct Yellow 12 by orange peel carbon, Desalination 238 (2009) 210–232.
[26] B.A. Bell, A.H. Molof, A new model of granular activated carbon adsorption kinetics, Water Res. 9 (1975) 857–860.
[27] L. Li, P.A. Quinlivan, D.R.U. Knappe, Effects of activated carbon surface chemistry and pore structure on the adsorption of organic contaminants from aqueous solution, Carbon 40 (2002) 2085–2100.
[28] S. Kasaoka, Y. Sakata, E. Tanaka, R. Naitoh, Design of molecular-sieve carbon. Studies on the adsorption of various dyes in the liquid phase, Int. Chem. Eng. 29 (1989) 734–742.
[29] C.H. Giles, T.H. MacEwan, S.N. Nakhwa, D. Smith, Studies in adsorption. Part XI. A system of classification of solution adsorption isotherms, and its use in diagnosis of adsorption mechanisms and in measurement of specific surface areas of solids, J. Chem. Soc. (1960) 3973–3993.
[30] F. Haghseresht, G.Q. Lu, Effects of acidic oxidation on the porosity of coal waste-derived chars, Carbon 37 (1999) 639–646.
[31] K. Kaneko, Determination of pore size and pore size distribution. 1. Adsorbents and catalysts, J. Membr. Sci. 96 (1994) 59–89.
[32] R.W. Magee, Evaluation of the external surface area of carbon black by nitrogen adsorption, Rubber Chem. Technol. 68 (1995) 590–599.
[33] S.J. Gregg, J.F. Langford, Study of the effect of compaction on the surface area and porosity of six powders by measurement of nitrogen sorption isotherms, J. Chem. Soc., Faraday Trans. 173 (1977) 747–759.
[34] S.J. Gregg, K.S.W. Sing, Adsorption, Surface Area and Porosity, Academic Press, London, 1982.
[35] J. Rouquerol, D. Avnir, C.W. Fairbridge, D.H. Everett, J.M. Haynes, N. Pernicone, J.D.F. Ramsay, K.S.W. Sing, K.K. Unger, Recommendations for the characterization of porous solids, Pure Appl. Chem. 66 (1994) 1739–1758.
[36] N.A. Medellin-Castillo, R. Leyva-Ramos, R. Ocampo-Perez, R.F.G. De La Cruz, A. Aragon-Pina, J.M. Martinez-Rosales, R.M. Guerrero-Coronado, L. Fuentes-Rubio, Adsorption of fluoride from water solution on bone char, Ind. Eng. Chem. Res. 46 (2007) 9205–9212.
[37] Y. Al-Degs, M.A.M. Khraisheh, S.J. Allen, M.N. Ahmad, Effect of carbon surface chemistry on the removal of reactive dyes from textile effluent, Water Res. 34 (2000) 927–935.